

# Top-Down Saliency Detection Driven by Visual Classification

Francesca Murabito   Concetto Spampinato   Simone Palazzo   Konstantin Pogorelov   Michael Riegler  
PeRCeiVeLab   PeRCeiVeLab   PeRCeiVeLab   Simula Research Lab   Simula Research Lab  
University of Catania   University of Catania   University of Catania   University of Oslo   University of Oslo

*Abstract*—This paper presents an approach for top-down saliency detection guided by visual classification tasks. We first learn how to compute visual saliency when a specific visual task has to be accomplished, as opposed to most state-of-the-art methods which assess saliency merely through bottom-up principles. Afterwards, we investigate if and to what extent visual saliency can support visual classification in nontrivial cases. To achieve this, we propose *SalClassNet*, a CNN framework consisting of two networks jointly trained: a) the first one computing top-down saliency maps from input images, and b) the second one exploiting the computed saliency maps for visual classification.

To test our approach, we collected a dataset of eye-gaze maps, using a Tobii T60 eye tracker, by asking several subjects to look at images from the Stanford Dogs dataset, with the objective of distinguishing dog breeds.

Performance analysis on our dataset and other saliency benchmarking datasets, such as POET, showed that *SalClassNet* outperforms state-of-the-art saliency detectors, such as *SalNet* and *SALICON*. Finally, we analyzed the performance of *SalClassNet* in a fine-grained recognition task and found out that it generalizes better than existing visual classifiers.

The achieved results, thus, demonstrate that 1) conditioning saliency detectors with object classes reaches state-of-the-art performance, and 2) providing explicitly top-down saliency maps to visual classifiers enhances classification accuracy.

*Index Terms*—visual attention, image classification, fully-convolutional neural networks

## I. INTRODUCTION

Computer vision and machine learning methods have long attempted to emulate humans while performing visual tasks. Despite the high intentions, the majority of the existing automated methods rely on a common schema, i.e., learning low- and middle-level visual features for a given task, often without taking into account the peculiarities of the task itself. One of the most relevant example of task-driven human process is visual attention, i.e., gating visual information to be processed by the brain according to the intrinsic visual characteristics of scenes (bottom-up process) and to the task to be performed (top-down process). In particular, bottom-up saliency mainly employs low-level visual cues, modeling unconscious vision processes, and shows huge limitations in task-oriented computer vision methods. For example, traditional bottom-up saliency methods [1] miss objects of interest in highly cluttered backgrounds since they detect visual stimuli, which often are unrelated to the task to be accomplished as shown in Fig. 1. Analogously, image classifiers fail in cases of cluttered



Fig. 1. **First column** — Eye fixations in free-viewing experiments in images with multiple objects. Some of the salient regions cannot be used for dog species classification. **Second Column** — Eye fixation shifts when asking to guess dog breeds.

images as they tend to extract low and middle level visual descriptors and match them with learned data distributions without focusing on the most salient image parts.

Under this scenario, the contribution of this paper is twofold: a) we present a method for saliency detection guided by a visual classification task; and b) we demonstrate that exploiting such task-based saliency maps improves the performance of classifiers. More specifically, we propose and train, in an end-to-end fashion, a convolutional neural network —

*SalClassNet* — consisting of two parts: the first one generating top-down saliency maps from input images, while the second one taking images and learned maps as input to perform visual categorization.

We tested the saliency detector of *SalClassNet* over challenging saliency datasets, where it significantly outperformed existing methods such as *SalNet* ([2]) and *SALICON* ([3]). In particular, we demonstrate how the propagation of a mixed saliency/classification loss throughout the upstream *SalClassNet* saliency detector is the key to learn task-guided saliency maps able to detect better the most discriminative features in the categorization process.

As for evaluating the performance of *SalClassNet* for visual categorization, we tested it on fine-grained classification tasks over, respectively, the Stanford Dogs ([4]), the CUB-200-2011 ([5]), and the Oxford Flower 102 ([6]) datasets, showing that explicitly providing visual classifiers with top-down saliency maps leads to better generalization performance.

As an additional contribution, we release our saliency dataset containing about 10,000 maps recorded from multiple users when performing a visual classification task on 120 Stanford Dogs fine-grained classes together with the *SalClassNet* Torch code and trained models.

## II. RELATED WORK

Visual attention in humans can be seen as the integration between a) an early bottom-up unconscious process where the attention is principally guided by some coarse visual stimuli, which can be local (e.g., center-surround mechanisms) or global (dependent from the context); and b) a late top-down process, which biases the observation towards those regions that consciously attract users’ attention according to a specific visual task. While the former has been extensively researched in the computer vision field with a significant number of proposed saliency detection methods ([7], [8], [3], [2], [9], [10], [11], [12], [13]), top-down processes have received much less attention ([14], [15], [16], [17]), mainly because of the greater difficulty to emulate high-level cognitive processes than low-level cues based on orientation, intensity and color ([1]). However, understanding the processes which are behind task-controlled visual attention may be of crucial importance to make machines see and understand the visual world as humans do as well as to solve complex vision tasks, such as recognition of multiple objects in cluttered scenes [18]. Recently, the rediscovery of convolutional neural networks and their high performance on visual tasks have led to the development of deep saliency detection networks that either adopt multi-scale patches for global/coarser and local/finer features extraction for further saliency assessment ([9], [10], [12], [11], [19], [13], [7], [3], [10], [20], [21], [12], [22], [23]) or learn, in an end-to-end fashion, saliency maps as in ([3], [2], [24]). In particular, the recently-published ([2]) presents an attempt of training an end-to-end fully-convolutional CNN (partly from scratch and partly by re-using low-level layers

from existing models) for saliency prediction; another fully-convolutional architecture is the one presented in ([3]), which processes images at two different scales and is based on deep neural networks trained for object recognition; the latter was used as basis for our work as described later.

Lately, the idea of using saliency for improving classification performance has gained significant attention from the computer vision community, coming up with saliency detection models that have been integrated into visual classification methods. In ([25]), saliency maps are employed to weigh features both in the learning and in the representation steps of a sparse coding process, whereas in ([26]) CNN-based part detections are encoded via Fisher Vectors and the importance of each descriptor is assigned through a saliency map. Ba et al. ([27]) extended the recurrent attention model (RAM) presented in ([28]) (a model based on a combination between recurrent neural networks and reinforcement learning to identify *glimpse* locations) by training it to detect and classify objects after identifying a fixed number of glimpses. Similarly, recent saliency detection methods have been fed with high level information in order to extract top-down attention maps. In ([29]), given the class label as prior, the parameters of a new feedback layer are learned to optimize the target neuron output by filtering out noisy signals; in ([30]) a new backpropagation scheme, “Excitation Backprop”, based on a probabilistic version of the Winner-Take-All principle, is introduced to identify task-relevant neurons for weakly-supervised localization. Our top-down saliency maps differ from the ones computed by those methods since the only top-down signal introduced in our training is a class-agnostic classification loss; hence, our maps are able to highlight those areas which are relevant for classifying generic images. A work similar in the spirit to ours is ([31]), where a low-capacity network initially scans the input image to locate salient regions using a gradient entropy with respect to feature vectors; then, a high-capacity network is applied to the most salient regions and, finally, the two networks are combined through their top layers in order to classify the input image. Our objective, however, is to perform end-to-end training, so that the classification error gradient can directly affect the saliency generation process. Given these premises, the most interesting saliency network architectures for our purpose are the ones which are fully-convolutional and whose output can be seamlessly integrated into a larger framework with a cascading classification module. Tab. I summarizes the results of state-of-the-art fully-convolutional saliency networks on a set of commonly-employed datasets for saliency detection benchmarking, namely *SALICON* validation and test sets ([3]), *iSUN* validation and test sets ([32]) and *MIT300* ([33]). In this work, we focus our attention, both as building blocks and evaluation baselines, on the *SALICON* ([3]) and *SalNet* ([2]) models, thanks to code availability and their fully-convolutional nature.

Method	N. Layers	Framework	Training Dataset	Fine-tuned	SALICON Test	SALICON Val	iSUN Test	iSUN Val	MIT300
<b>JuntingNet</b>	5	Lasagne	SALICON	No	CC = 0.60 Shuffled-AUC = 0.67 AUC Borji = 0.83	CC = 0.58 Shuffled-AUC = 0.67 AUC Borji = 0.83	CC = 0.82 Shuffled-AUC = 0.67 AUC Borji = 0.85	CC = 0.59 Shuffled-AUC = 0.64 AUC Borji = 0.79	CC = 0.53 Shuffled-AUC = 0.64 AUC Borji = 0.78
<b>SalNet</b>	10	Caffe	SALICON	No	CC = 0.62 No Shuffled-AUC = 0.72 AUC Borji = 0.86	CC = 0.61 Shuffled-AUC = 0.73 AUC Borji = 0.86	CC = 0.62 Shuffled-AUC = 0.72 AUC Borji = 0.86	CC = 0.53 Shuffled-AUC = 0.63 AUC Borji = 0.80	CC = 0.58 Shuffled-AUC = 0.69 AUC Borji = 0.82
<b>SALICON</b>	16	Caffe	OSIE	No	—	—	—	—	CC = 0.74 Shuffled-AUC = 0.74 AUC Borji = 0.85
<b>DeepGaze</b>	5	Not Available	MIT1003	No	—	—	—	—	CC = 0.48 Shuffled-AUC = 0.66 AUC Borji = 0.83
<b>DeepGaze 2</b>	19	Web Service	SALICON - MIT1003	No	—	—	—	CC = 0.51 Shuffled-AUC = 0.77 AUC Borji = 0.86	—
<b>ML-NET</b>	19 + 2	Theano	SALICON	Yes	CC = 0.76 Shuffled-AUC = 0.78	—	—	—	CC = 0.69 Shuffled-AUC = 0.70 AUC Borji = 0.77
<b>DeepFix</b>	20	Not Available	SALICON	Yes	—	—	—	—	CC = 0.78 Shuffled-AUC = 0.71 AUC Borji = 0.80
<b>eDN</b>	Ensemble	Sthor	MIT1003	No	—	—	—	—	CC = 0.45 Shuffled-AUC = 0.62 AUC Borji = 0.81
<b>PDP</b>	16 + 3	Not Available	SALICON	Yes	CC = 0.77 Shuffled-AUC = 0.78 AUC Borji = 0.88	CC = 0.74 Shuffled-AUC = 0.78	—	—	CC = 0.70 Shuffled-AUC = 0.73 AUC Borji = 0.80

TABLE I

A SUMMARY OF STATE-OF-ART FULLY-CONVOLUTIONAL METHODS AND THEIR RESULTS, ACCORDING TO THE MOST COMMON METRICS, ON SEVERAL SALIENCY DATASETS. DATASETS (LEFT TO RIGHT): **SALICON TEST** ([34]), **SALICON VAL** ([34]), **iSUN TEST** ([32]), **iSUN VAL** ([32]), **MIT300** ([33]). METHODS (TOP-BOTTOM): **JUNTINGNET** ([2]), **SALNET** ([2]), **SALICON** ([3]), **DEEPGAZE** ([8]), **DEEPGAZE2** ([35]), **ML-NET** ([36]), **DEEPLIT** ([37]), **EDN** ([38]), **PDP** ([39])

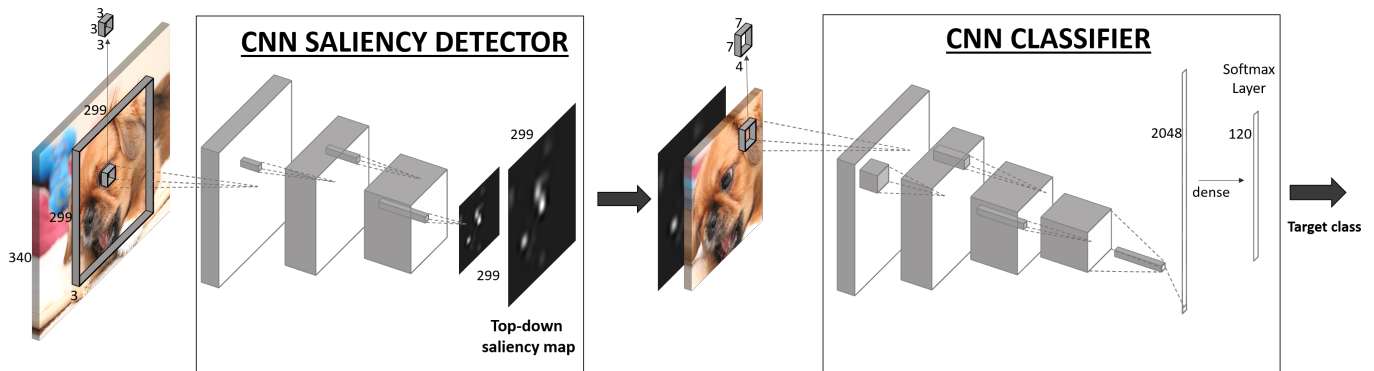


Fig. 2. Architecture of the proposed model – *SalClassNet*– for saliency detection guided by a visual classification task. Input images are processed by a saliency detector, whose output together with input images are fed to a classification network with 4-channel first-layer kernels for processing image color and saliency and providing image classes as output.

### III. SALCLASSNET: A CNN MODEL FOR TOP-DOWN SALIENCY DETECTION

The general architecture of our network is shown in Fig. 2 and is made up of two cascaded modules: a saliency detector and a visual classifier, which are jointly trained in a multi-loss framework.

#### A. Top-down saliency detection network

Although we will discuss the details of the employed saliency dataset and its generation process in Sect. IV, it is necessary to introduce some related information at this stage, which is important to understand the overall model.

In the dataset generation protocol, human subjects were explicitly asked to look at a computer screen showing images and try to guess the classes of specific objects (e.g., dog breeds). Therefore, our experiments aimed to enforce top-down saliency driven by a specific classification task, rather

than bottom-up saliency. In other words, instead of emphasizing the location of image regions which are visually interesting per se (which, of course, may include the target object), our saliency maps focus on the location of features needed for identifying the target classes, ignoring everything else, which may be salient but not relevant to the classification task. Hence, our saliency detector has to be able, given an input image, to produce a map of the most salient image locations useful for classification purposes.

To accomplish that, we propose a CNN-based saliency detector composed by thirteen convolutional and five max pooling layers taken from VGG-16 ([40]). The output of the last pooling layer, i.e.,  $512 \times 10 \times 10$  feature maps (for a  $3 \times 299 \times 299$  input image), is then processed by a  $1 \times 1$  convolution to compute a saliency score for each “pixel” in the feature maps of the previous layer, producing a single-channel map. Finally, the obtained saliency map is transformed into a  $299 \times 2099$  saliency map through an upsampling layer followed by a

convolutional layer in order to generate the input to the subsequent classification network.

### B. Saliency-based classification network

Our visual classifier is a convolutional neural network which receives as input a 4-channel RGBS image, combining the RGB image with the corresponding saliency (S) map, and provides as output the corresponding class. The underlying idea is that the network should employ those salient regions (as indicated by the input saliency map S) more meaningful for classification purposes.

This network is based on a pretrained Inception network ([41]) which comprises sixteen convolutional and one fully connected layers followed by a final softmax layer, with the first-layer convolutional kernels modified to support the 4-channel input (image plus its saliency map coming from the saliency subnetwork). In particular, the 32  $3 \times 3 \times 3$  kernels in the first layer are converted into 32  $4 \times 3 \times 3$  kernels, whose weights corresponding to the RGB channels are taken from the pretrained Inception network, whereas the new weights, corresponding to the saliency input, are randomly initialized. Since the model includes a combination of trained weights (the ones from the original Inception) and untrained weights (the ones related to the saliency channel) we set different learning rates in order to speed up the convergence of untrained weights while not destabilizing the already learned ones.

### C. Multi-loss saliency-classification training

The networks, described in the previous sections, are joined together into a single sequential model and trained using RGB images as input and corresponding class labels as output. We introduced a batch normalization module between the saliency detector and the classifier, to enforce a zero-mean and unitary-standard-deviation distribution at the classifier’s input. During training, we minimize a multi-loss objective function given by a linear combination of cross-entropy classification loss  $\mathcal{L}_C$ , and saliency detector loss  $\mathcal{L}_S$  computed as the mean square error of the intermediate saliency detector’s output with respect to the ground-truth heatmap for the corresponding input image:

$$\mathcal{L}(\mathbf{y}, \mathbf{Y}, t, \mathbf{T}) = \alpha \mathcal{L}_C(\mathbf{y}, t) + \mathcal{L}_S(\mathbf{Y}, \mathbf{T}) \quad (1)$$

where

$$\mathcal{L}_C(\mathbf{y}, t) = - \sum_{i=1}^n \mathbb{I}(i = t) \log(y_i) \quad (2)$$

$$\mathcal{L}_S(\mathbf{Y}, \mathbf{T}) = \frac{1}{hw} \sum_{i=1}^h \sum_{j=1}^w (Y_{ij} - T_{ij})^2 \quad (3)$$

where  $\mathcal{L}_C$  is the cross-entropy loss computed for the softmax output vector  $\mathbf{y}$  and the correct class  $t$ ,  $n$  indicates the number classes in the dataset,  $\mathcal{L}_S$  is the mean square error loss computed on the saliency detector’s output map  $\mathbf{Y}$  and the ground-truth heatmap  $\mathbf{T}$ ,  $h$  and  $w$  represent the size of this heatmap, and  $\mathbb{I}(p)$  is the indicator function, which returns 1 if  $p$  is true; bold symbols denote vectors (lower case) and matrices (upper case).

The adopted multi-loss affects the model in several ways. First of all, backpropagating the classification loss to the saliency detector forces it to learn saliency features useful for classification. Secondly, backpropagating the mean square error on the saliency maps ensures that the saliency detector does not degenerate into identifying generic image features and become a convolutional layer as any other.

Fig. 3 shows two output examples of how saliency changes when using only saliency losses  $\mathcal{L}_S$  to train the saliency detector and when driving it by the classification loss  $\mathcal{L}_C$ : the saliency shifted from generic scene elements to more discriminative features.

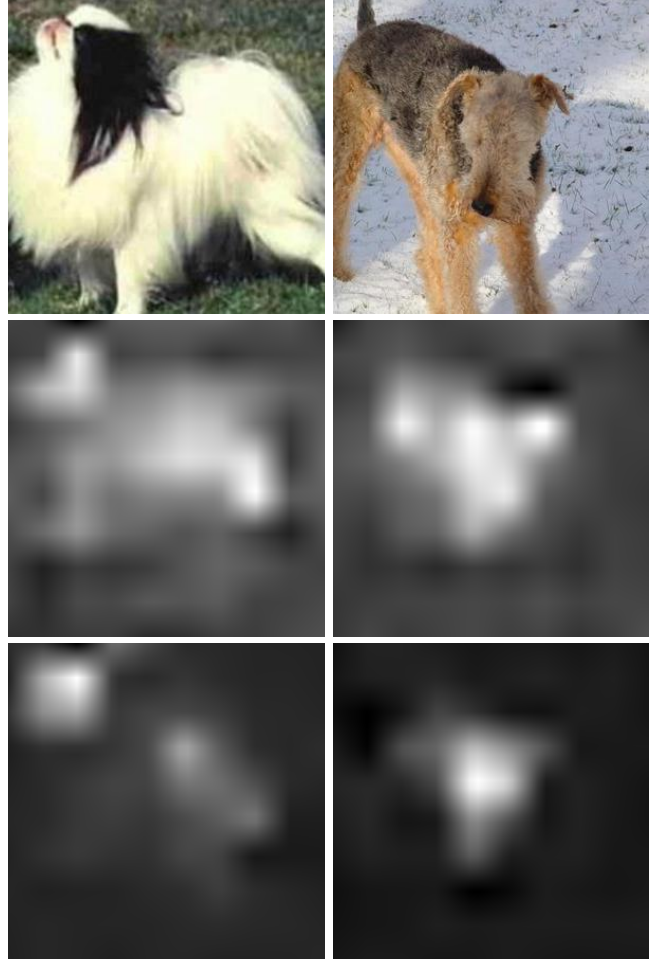


Fig. 3. **From bottom-up to top-down saliency maps.** (Top row) Two example images. (Middle row) Bottom-up saliency maps generated by our CNN-based saliency detector fine-tuned over the Stanford Dog dataset using ground-truth heatmaps. (Bottom row) Shift of saliency guided by the classification task, as resulting from training SalClassNet.

## IV. TOP-DOWN SALIENCY DATASET

To test our saliency detector, we built a top-down saliency dataset consisting of eye-gaze data recorded from multiple human subjects while observing dog images taken from the Stanford Dogs dataset ([4]), a collection of 20,580 images of dogs from 120 breeds (about 170 images per class). From

the whole Stanford Dogs dataset, we used a subset of 9,861 images keeping the original class distribution. The eye-gaze acquisition protocol involved 12 users, who were asked to look at the images shown on a computer screen and attempt to identify dog breeds. To enforce top-down saliency, images were initially blurred and gradually enhanced until subjects were able to recognize the dog breeds. Thus, each image was shown the time needed by the subjects to identify breeds and eye-gaze were recorded through a 60-Hz Tobii T60 eye-tracker. Tab. II shows a summary of the dataset’s statistics. To the best of our knowledge, this is one the first publicly-available datasets featuring saliency maps driven by visual classification tasks, and the first one dealing with a large number of fine-grained object classes, thus making the saliency detection problem more complex.

	Our Dataset
Number of images	9,861
Number of classes	120
Avg. number of images per class	82.2
Avg. number of fixation points per image	6.2

TABLE II  
INFORMATION ON THE GENERATED SALIENCY DATASET.

A dataset similar to ours has been recently proposed in ([42]), however, it does not deal with fine-grained classification tasks, but with classification at the basic level and with fewer classes (10 Pascal VOC classes vs 120 of our case). Tab. III reports a comparison, in terms of enforced attention mechanism (e.g., tasks accomplished by participants), number of viewers, collected images and acquisition devices, between our dataset and recent saliency benchmarking datasets, namely, SALICON ([3]), iSUN ([32]), MIT300 ([33]) and POET([42]).

Beside being the first saliency dataset linked to a fine-grained visual classification task, the saliency maps of our dataset are very accurate since there were generated using a Tobii T60 eye tracker whose gaze detection accuracy is known to be higher (error < 2mm regardless the position/distance from the device) than camera and video-based ones.

## V. PERFORMANCE ANALYSIS

The performance analysis is organized as follows: a) first, we tested the quality of the saliency maps generated by the proposed method and compared it to other saliency detectors over our eye-gaze dataset and the POET dataset; b) then, we investigated whether exploiting saliency maps (top-down vs bottom-up) would increase classification performance in fine-grained visual recognition tasks or not.

### A. Datasets and training settings

**Datasets.** For testing saliency detection performance, we split our dataset (9,861 images with heatmaps) into training set (80%, 8,005 images), validation set (10%, 928 images) and test set (10%, 928 images). We also tested the generalization capabilities of SalClassNet over the POET dataset.

For visual classification performance, we first investigated the contribution of saliency on visual classification over our

dataset (using the split described above). Then, to ground SalClassNet to the state of the art on fine-grained image classification, we defined a “de-duped” version of the dog image dataset consisting of 6,000 images taken from the ImageNet validation set, uniformly distributed over the 120 dog breed classes. This was done to carry out a fair comparison between visual classifiers pretrained on ImageNet, such as Inception and VGG-16, and our method, since all the images available in the original version of Stanford Dogs were already contained in the ImageNet training set. Furthermore, the generalization capabilities of SalClassNet were tested on the CUB-200-2011 ([5]) and Oxford Flower 102 ([6]) datasets.

**Training settings.** During training, input images (and corresponding heatmaps, when appropriate) were resized so that the smallest image side was 340 pixels, by keeping the original aspect ratio. Data augmentation for training was performed by computing, for each image, five random crops and corresponding horizontal flips; given the fully-convolutional nature of the whole model, input size can be arbitrary: we used 299×299 image crops for input and output, using ground-truth heatmaps normalized to zero-mean and unitary-standard-deviation. During evaluation on the validation and test sets, only the central crop was employed.

As for training algorithm parameters, we performed gradient descent using SGD with a learning rate of 0.05 for network weights trained from scratch and of 0.001 for fine-tuning: learning rate decay factor was set to 0.00001, momentum to 0.9 and weight decay to 0.0005. Our saliency detector was pretrained on the OSIE dataset ([43]). The RGBS (RGB plus saliency) classifier (i.e., the classification network of SalClassNet), instead, was initially pretrained on the Stanford Dogs dataset together with ground-truth heatmaps; however, its parameters were frozen during the fine-tuning of the whole SalClassNet, when only the saliency detection sub-network was updated.

We did not set a fixed number of training epochs, but stopped when the validation accuracy did not improve for 10 consecutive epochs. In practice, all models converged in 70-120 epochs. Model selection was performed by maximizing the validation accuracy or by minimizing the MSE loss, depending on whether we were training a classifier or a saliency detector; for SalClassNet we chose to maximize the validation accuracy. For the multi-loss end-to-end training, we heuristically set the  $\alpha$  parameter in Eq. 1 to 0.01, given that saliency loss (MSE) was on average one order of magnitude greater than classification loss (cross-entropy).

### B. Saliency detection performance

To evaluate the capabilities of the top-down saliency detector of SalClassNet, we employed as metrics ([44]): shuffled area under curve (s-AUC), normalized scanpath saliency (NSS) and correlation coefficient (CC) scores, and compared its performance to those achieved, respectively, by the SALICON and SalNet models fine-tuned on our eye-gaze dataset for dog species classification.

Tab. IV reports a quantitative comparison between these ap-

Dataset	Capture method	Task	Viewers	Train	Validation	Test
SALICON ([34])	Mouse clicks	Free-viewing	Crowd	10,000	5,000	5,000
iSUN ([32])	Camera-based eye tracker	Free-viewing	Crowd	6,000	926	2,000
MIT300 ([33])	ISCAN video-based eye tracker	Free-viewing	39	-	-	-
POET ([42])	Eyelink 2000 eye tracker	Basic classification	28	441	-	5,829
Our dataset	Tobii T60 eye tracker	Fine-grained classification	12	8,005	928	828

TABLE III  
COMPARISON BETWEEN OUR DATASET AND STATE OF THE ART ONES

Method	s-AUC	NSS	CC
<b>Dataset</b>	<b>Our dataset</b>		
SALICON	0.720	2.106	0.408
SalNet	0.703	2.182	0.400
SalClassNet	<b>0.771</b>	<b>2.364</b>	<b>0.434</b>
<b>Dataset</b>	<b>POET dataset</b>		
SALICON	0.634	1.232	0.289
SalNet	0.649	1.093	0.300
SalClassNet	<b>0.653</b>	<b>1.405</b>	<b>0.315</b>

TABLE IV  
COMPARISON IN TERMS OF SHUFFLED AREA UNDER CURVE (S-AUC), NORMALIZED SCANPATH SALIENCY, CORRELATION COEFFICIENT (CC) BETWEEN THE SALICON, SALNET AND SALCLASSNET: A) TRAINED (OR FINE-TUNED) ON OUR DATASET’S GROUND-TRUTH HEATMAPS, AND B) TESTED ON POET DATASET

proaches (fine-tuned) over our dataset and the POET dataset, which was used as additional benchmark since its saliency maps are similar to ours (i.e., they are computed through eye gaze data collected on a classification dataset). It is possible to notice that SalClassNet is able to generate more accurate (and generalizes better) top-down saliency maps than existing methods, which suggests that driving the generation of saliency maps with a specific goal, indeed, leads to better performance than fine-tuning already-trained models (beside being less time consuming). Fig. 4 and 5 report some output examples of the tested methods on different input images from our dataset and other image datasets (POET, CUB200-2011 and Flower102), respectively. These qualitative results show SalClassNet’s capabilities to generalize well the top-down saliency detection process even across different datasets.

### C. Effect of saliency maps on visual classification performance

In the previous section, we showed the quality of the top-down saliency generation process, while in this section, we investigate if, and to what extent, providing explicitly saliency maps can contribute to improve classification performance. To this end, we first assessed the performance of VGG-19 ([40]) and Inception ([41]) over the fine-grained Stanford Dogs dataset when using a) only color images (3-channel models) and b) saliency maps (ground-truth, i.e., the ones available in our eye gaze dataset) plus color images (4-channel models). Both 3 and 4 channel versions of Inception and VGG-19 were fine-tuned over the Stanford Dogs dataset. Results, in terms of mean classification accuracy, are reported in Tab. V

Method	MCA
VGG ([40]) (3 channels)	56.1%
VGG (4 channels) + ground truth saliency maps	57.4%
Inception ([41]) (3 channels)	80.4%
Inception (4 channels) + ground truth saliency maps	82.1%

TABLE V  
COMPARISON IN TERMS OF MEAN CLASSIFICATION ACCURACY BETWEEN THE ORIGINAL INCEPTION AND VGG MODELS FINE-TUNED ON THE STANFORD DOG DATASET AND THEIR RGBS VARIANTS TRAINED ON GROUND-TRUTH SALIENCY HEATMAPS.

Method	MCA
VGG ([40]) (3 channels)	45.0%
Inception ([41]) (3 channels)	82.0%
SalClassNet	79.9%

TABLE VI  
COMPARISON IN TERMS OF MEAN CLASSIFICATION ACCURACY BETWEEN THE ORIGINAL INCEPTION AND VGG MODELS AND THE PROPOSED SALCLASSNET OVER THE “DE-DUPED” DOG IMAGE DATASET.

and show that providing accurate saliency information to traditional visual classifier yields to improved performance.

However, although eye-tracker systems will likely be embedded in mobile devices in the near future, it is still unfeasible to assume the availability of ground-truth saliency maps every time visual classification on a new image has to be performed; thus, we tested SalClassNet, which automatically generates saliency maps and uses them for classification, and compared it to the aforementioned methods over the “de-duped” dog image dataset previously described. As explained in the previous section, the “de-duped” dog image dataset was employed in order to make a fair comparison between SalClassNet, when used as visual classifier, and other models already pre-trained on the Stanford Dog Dataset (which is part of the ImageNet training set). Tab. VI shows the achieved mean classification accuracies for all the tested methods. SalClassNet achieved state of the art performance (comparable to Inception’s and sensibly better than VGG-16’s). Its slightly lower classification accuracy value with respect to Inception’s one might be due a) to the effort to replicate correctly top-down saliency maps while preserving classification accuracy, and b) to the fact that Inception, when trained on an image dataset, internally learns also saliency maps, resulting in good results on data coming from the same training data distribution.

Nevertheless, SalClassNet when tested on completely different scenarios showed better generalization capabilities than

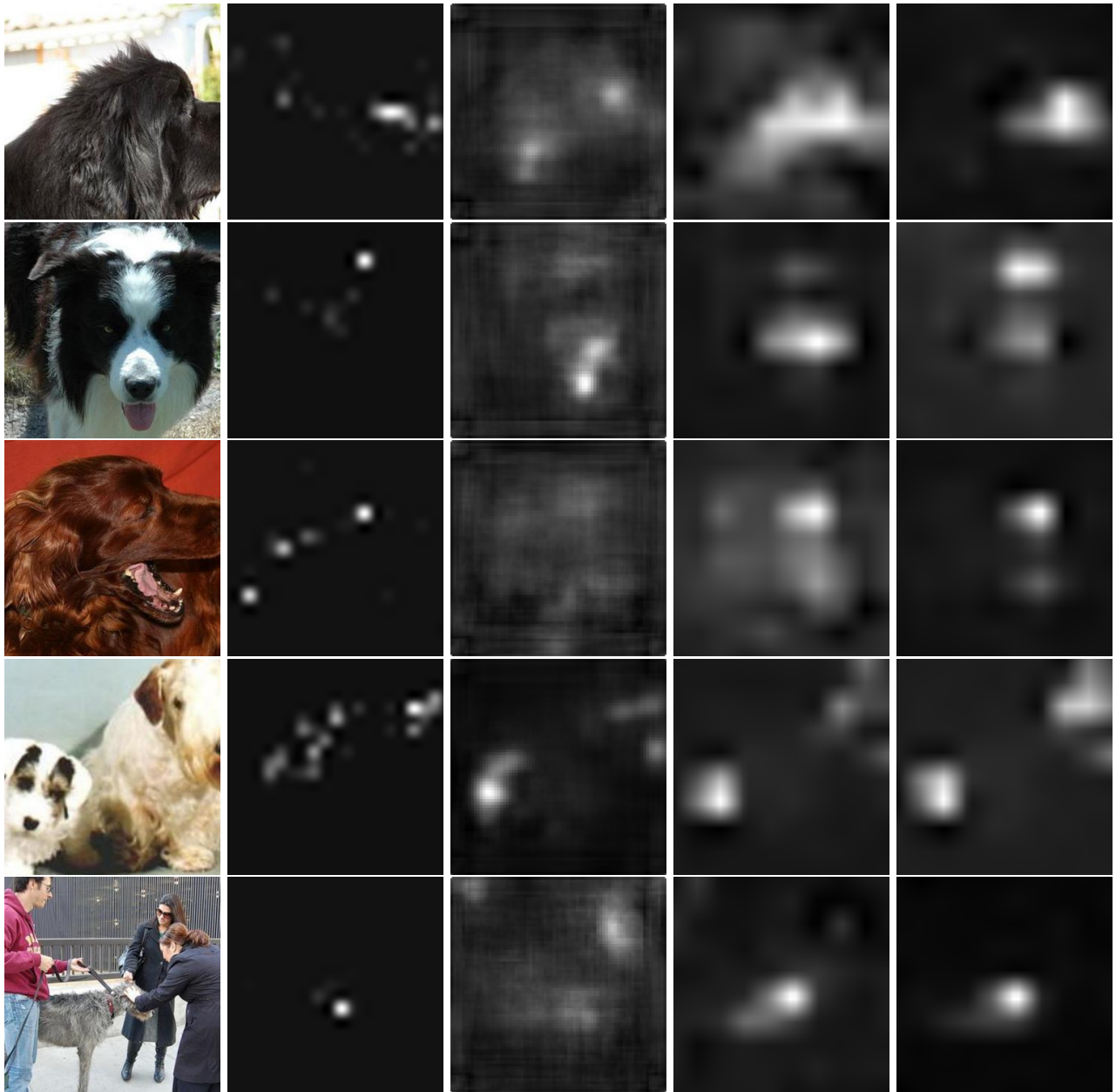


Fig. 4. **Comparison of saliency output maps from different methods.** Each row, from left to right, shows an example image, the corresponding ground-truth top-down saliency maps, and the output maps computed, in order, by SalNet (fine-tuned on ground-truth heatmaps), SALICON (fine-tuned on ground-truth heatmaps), and the proposed end-to-end SalClassNet model. Beside being able to identify those areas which can be useful for recognition (see first three rows), our method can highlight multiple salient objects (both dogs in the fourth row), or suppress those objects which are not salient for the task (see fifth row)

Inception. In particular, we tested SalClassNet over two other fine-grained dataset, CUB-200-2011 and Oxford Flower 102, by employing SalClassNet as a feature extractor for a softmax classifier. Its results were compared to those achieved, on the same datasets, by Inception and VGG-19 (also employed as feature extractors followed by a softmax classifier, as in our case) and are shown in Tab. VII confirming our previous claim.

## VI. CONCLUDING REMARKS

In this work, we proposed a deep architecture — SalClassNet — which generates top-down saliency maps by conditioning, through the object class supervision, the saliency detection process and, at the same time, exploits such saliency maps for visual classification. Performance analysis showed that the method identifies regions corresponding to class-discriminative features, hence emulating top-down saliency, unlike existing saliency detection approaches which produce bottom-up maps of generic salient visual features. Although



Fig. 5. Examples of top-down saliency maps generated by SalClassNet on **CUB-200-2011** (first row) **Oxford Flower 102** (second row) and **POET** (third row) and compared to SALICON-generated saliency maps. SalClassNet is able to detect the most distinctive features needed for visual classification, while SALICON identifies all salient areas (e.g., branch under the rusty blackbird — first row, third column).

	<b>CUB-200-2011</b>	<b>Oxford Flower 102</b>
<b>Method</b>		
VGG	50.1%	64.7%
Inception	64.7%	77.6%
SalClassNet	<b>65.4%</b>	<b>78.5%</b>

TABLE VII

PERFORMANCE OBTAINED BY VGG, INCEPTION AND SALCLASSNET OVER, RESPECTIVELY, **CUB-200-2011** AND **OXFORD FLOWER 102**

we tested our framework using two specific networks for saliency detection and visual classification, its architecture and our software implementation are general and can be used with any fully-convolutional saliency detector or classification network by simply replacing one of the two subnetworks, respectively, before or after the connecting batch normalization module. As further contribution of this paper, we built a dataset of saliency maps (by means of eye-gaze tracking experiments on 12 subjects who were asked to guess dog breeds) for a subset of the Stanford Dog dataset, creating what is, to the best of our knowledge, the first publicly-available top-down saliency dataset driven by a fine-grained visual classification task. We hope that our flexible deep network architecture (all source code is available) together with our eye-gaze dataset will push the research in the direction of emulating human visual processing through a deeper understanding of higher-level (such as top-down visual attention) processes behind it.

## REFERENCES

- [1] L. Itti, C. Koch, A saliency-based search mechanism for overt and covert shifts of visual attention, *Vision Research* 2000 (2000) 1489–1506.
- [2] J. Pan, E. Sayrol, X. Giro-i Nieto, K. McGuinness, N. E. O’Connor, Shallow and deep convolutional networks for saliency prediction, in: *CVPR* 2016, 2016.
- [3] X. Huang, C. Shen, X. Boix, Q. Zhao, Salicon: Reducing the semantic gap in saliency prediction by adapting deep neural networks, in: *ICCV* 2015, 2015, pp. 262–270.
- [4] A. Khosla, N. Jayadevaprakash, B. Yao, L. Fei-Fei, Novel dataset for fine-grained image categorization, in: *CVPRW* 2011, 2011.
- [5] C. Wah, S. Branson, P. Welinder, P. Perona, S. Belongie, The Caltech-UCSD Birds-200-2011 Dataset.
- [6] M.-E. Nilsback, A. Zisserman, Automated flower classification over a large number of classes, in: *ICVGIP* 2008, 2008.
- [7] G. Li, Y. Yu, Visual saliency detection based on multiscale deep CNN features, *Transactions on Image Processing* 2016 (2016) 5012–5024.
- [8] M. Kummerer, L. Theis, M. Bethge, Deep Gaze I: Boosting saliency prediction with feature maps trained on imagenet, in: *ICLRW* 2015, 2015.
- [9] S. He, R. W. H. Lau, W. Liu, Z. Huang, Q. Yang, SuperCNN: A superpixelwise convolutional neural network for salient object detection, *IJCV* 2015 (2015) 330–344.
- [10] N. Liu, J. Han, D. Zhang, S. Wen, T. Liu, Predicting eye fixations using convolutional neural networks, in: *CVPR* 2015, 2015.
- [11] G. Li, Y. Yu, Visual saliency based on multiscale deep features, in: *CVPR* 2015, 2015.
- [12] R. Zhao, W. Ouyang, H. Li, X. Wang, Saliency detection by multi-context deep learning, in: *CVPR* 2015, 2015, pp. 1265–1274.

- [13] J. Han, D. Zhang, S. Wen, L. Guo, T. Liu, X. Li, Two-stage learning to predict human eye fixations via sdaes, *Transaction on Cybernetics* 2016 (2016) 487–498.
- [14] R. J. Peters, L. Itti, Beyond bottom-up: Incorporating task-dependent influences into a computational model of spatial attention, in: 2007 IEEE Conference on Computer Vision and Pattern Recognition, 2007, pp. 1–8. doi:10.1109/CVPR.2007.383337.
- [15] T. Judd, K. Ehinger, F. Durand, A. Torralba, Learning to predict where humans look, in: 2009 IEEE 12th International Conference on Computer Vision, 2009, pp. 2106–2113.
- [16] L. Itti, Probabilistic learning of task-specific visual attention, in: Proceedings of the 2012 IEEE Conference on Computer Vision and Pattern Recognition (CVPR), CVPR '12, 2012, pp. 470–477.
- [17] G. Zhu, Q. Wang, Y. Yuan, Tag-saliency: Combining bottom-up and top-down information for saliency detection, *Computer Vision and Image Understanding* 118 (2014) 40 – 49.
- [18] D. Walther, U. Rutishauser, C. Koch, P. Perona, Selective visual attention enables learning and recognition of multiple objects in cluttered scenes, *Computer Vision and Image Understanding* 100 (1) (2005) 41 – 63.
- [19] Y. Lin, S. Kong, D. Wang, Y. Zhuang, Saliency detection within a deep convolutional architecture, in: AAAIW, 2014.
- [20] C. Shen, Q. Zhao, Learning to predict eye fixations for semantic contents using multi-layer sparse network, *Neurocomputing* 2014 (2014) 61 – 68.
- [21] L. Wang, H. Lu, X. Ruan, M. H. Yang, Deep networks for saliency detection via local estimation and global search, in: CVPR 2015, 2015, pp. 3183–3192.
- [22] Y. Tang, X. Wu, Saliency detection via combining region-level and pixel-level predictions with cnns, in: ECCV 2016, 2016, pp. 809–825.
- [23] T. Chen, L. Lin, L. Liu, X. Luo, X. Li, Disc: Deep image saliency computing via progressive representation learning, *Transaction on NNLS* 2016 (2016) 1135–1149.
- [24] G. Li, Y. Yu, Deep contrast learning for salient object detection, in: CVPR 2016, 2016.
- [25] Z. Ren, S. Gao, L.-T. Chia, I. W.-H. Tsang, Region-based saliency detection and its application in object recognition, in: TCSVT 2015.
- [26] X. Zhang, H. Xiong, W. Zhou, W. Lin, Q. Tian, Picking deep filter responses for fine-grained image recognition, in: CVPR 2016, 2016.
- [27] J. Ba, V. Mnih, K. Kavukcuoglu, Multiple object recognition with visual attention, in: ICLR 2015.
- [28] V. Mnih, N. Heess, A. Graves, k. kavukcuoglu, Recurrent models of visual attention, in: NIPS 2014, 2014, pp. 2204–2212.
- [29] C. Cao, X. Liu, Y. Yang, Y. Yu, J. Wang, Z. Wang, Y. Huang, L. Wang, C. Huang, W. Xu, et al., Look and think twice: Capturing top-down visual attention with feedback convolutional neural networks, in: CVPR 2015, 2015, pp. 2956–2964.
- [30] J. Zhang, Z. Lin, J. Brandt, X. Shen, S. Sclaroff, Top-down neural attention by excitation backprop, in: ECCV 2016, 2016, pp. 543–559.
- [31] A. Almahairi, N. Ballas, T. Cooijmans, Y. Zheng, H. Larochelle, A. Courville, Dynamic capacity networks, in: ICML 2016.
- [32] P. Xu, K. A. Ehinger, Y. Zhang, A. Finkelstein, S. R. Kulkarni, J. Xiao, Turkergaze: crowdsourcing saliency with webcam based eye tracking, arXiv preprint arXiv:1504.06755.
- [33] Z. Bylinskii, T. Judd, A. Borji, L. Itti, F. Durand, A. Oliva, A. Torralba, Mit saliency benchmark.
- [34] M. Jiang, S. Huang, J. Duan, Q. Zhao, Salicon: Saliency in context, in: CVPR 2015, 2015, pp. 1072–1080.
- [35] M. Kümmerer, T. S. Wallis, M. Bethge, Deepgaze ii: Reading fixations from deep features trained on object recognition, arXiv preprint arXiv:1610.01563.
- [36] M. Cornia, L. Baraldi, G. Serra, R. Cucchiara, Multi-level net: A visual saliency prediction model, in: ECCVW 2016, 2016, pp. 302–315.
- [37] S. S. Kruthiventi, K. Ayush, R. V. Babu, Deepfix: A fully convolutional neural network for predicting human eye fixations, IP 2017.
- [38] E. Vig, M. Dorr, D. Cox, Large-scale optimization of hierarchical features for saliency prediction in natural images, in: CVPR 2014, 2014, pp. 2798–2805.
- [39] S. Jetley, N. Murray, E. Vig, End-to-end saliency mapping via probability distribution prediction, in: CVPR 2016, 2016, pp. 5753–5761.
- [40] K. Simonyan, A. Zisserman, Very deep convolutional networks for large-scale image recognition, ICLR 2015 abs/1409.1556.
- [41] C. Szegedy, W. Liu, Y. Jia, P. Sermanet, S. Reed, D. Anguelov, D. Erhan, V. Vanhoucke, A. Rabinovich, Going deeper with convolutions, in: CVPR 2015, 2015.
- [42] D. P. Papadopoulos, A. D. Clarke, F. Keller, V. Ferrari, Training object class detectors from eye tracking data, in: ECCV 2014, 2014, pp. 361–376.
- [43] J. Xu, M. Jiang, S. Wang, M. S. Kankanhalli, Q. Zhao, Predicting human gaze beyond pixels, *JoV* 2014 (2014) 1–20.
- [44] A. Borji, D. N. Sihite, L. Itti, Quantitative analysis of human-model agreement in visual saliency modeling: A comparative study, *TIP*.